Application Note

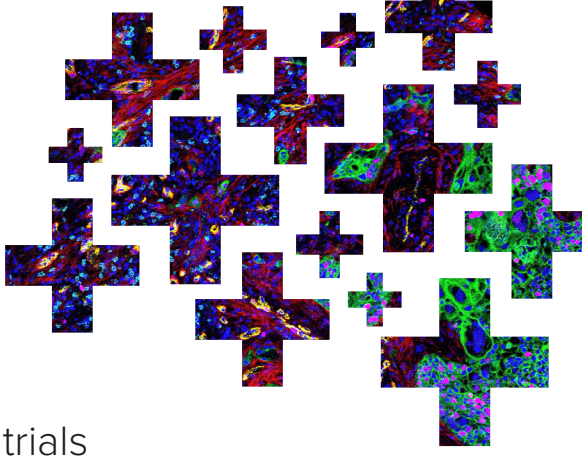

Hyperion+ Imaging System

Map spatial interactions from discovery to clinical trials twice as fast with this second-generation system

Introduction

The Hyperion™ Imaging System is a powerful tool in the study of complex cellular interactions in the tissue microenvironment and in the discovery of biomarkers that can predict disease outcome or response to therapy. It uses the power of Imaging Mass Cytometry™ (IMC™) to simultaneously examine 40-plus protein markers at subcellular resolution without spectral overlap or background autofluorescence, thus enabling researchers to gain new insights from precious tissue samples and microarrays.

The Hyperion+™ Imaging System is setting the new standard in spatial biology by empowering users to acquire data faster, with an improvement in the limit of detection, while maintaining image quality and rigor of data analysis. Table 1 lists the new features of the Hyperion+ Imaging System as compared with the original Hyperion Imaging System.

Objectives

This application note compares IMC data acquired on the Hyperion+ Imaging System vs. the Hyperion Imaging System to showcase the power of high-plex imaging at faster throughput. The results demonstrate:

- Better signal-to-noise ratio (S:N) of several markers
- Preservation of image quality and rigor of data analysis

Feature		Hyperion Imaging System	Hyperion+ Imaging System
Laser		Standard	Longer life
Ablation frequency		200 Hz	400 Hz
Ablation chamber gas		Helium	Hydrogen/ helium
ROI* size (µm) and acquisition time	500 x 500	25 min	15 min
	800 x 800	1 hr 1 min	35 min
	1,000 x 1,000	1 hr 35 min	54 min
Limit of detection		≥400 antibody copies per µm²	≥250 antibody copies per µm²
Number of unique markers (identified simultaneously)		≥40	≥40
Resolution		1 µm	1 µm
Software		CyTOF® Software v7.0	CyTOF Software v7.1

* Region of interest

Table 1. Hyperion and Hyperion+ Imaging System features

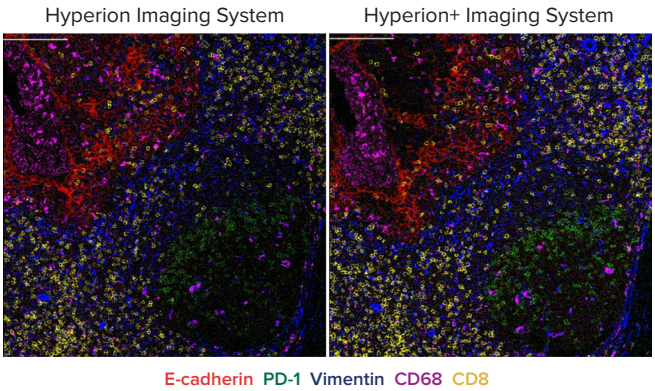

Figure 1. Equivalent image quality on Hyperion and Hyperion+ Imaging Systems. Serial sections of FFPE Human Chronic Tonsillitis tissue were stained with an antibody panel (Table 2) and matching ROIs were ablated using the Hyperion and Hyperion+ Imaging Systems. Global thresholding is applied to each channel. ROI size = 750 µm x 750 µm. Scale bar = 150 µm.

Study design

Tissue slides and panel design

Three formalin-fixed, paraffin-embedded (FFPE) human tissue slides – Chronic Tonsillitis, Lymph Node Tumor and Prostate Cancer (see Materials) – showing different expression levels of immune and structural markers were stained with optimized concentrations of the antibody panel shown in Table 2. The panel is a customized version of the Maxpar® Human Immuno-Oncology IMC Panel Kit (Cat. No. 201508). It was easily modified to include CD11b, CD31, LAG3 and the IMC Cell Segmentation Kit (ICSK, PN TIS-00001) while excluding CD20, Ki-67 and histone 3 for the purpose of this study.

Metal	Marker	Dilution	Cat. No.
141Pr	α-SMA	1:400	3141017D
143Nd	Vimentin	1:300	3143027D
148Nd	Pan-keratin	1:200	3148020D
149Sm	CD11b*	1:100	3149028D
150Nd	PD-L1	1:50	3150033D
151Eu	CD31*	1:100	3151025D
152Sm	CD45	1:200	3152018D
153Eu	LAG-3*	1:50	3153028D
155Gd	FoxP3	1:50	3155018D
156Gd	CD4	1:50	3156033D
158Gd	E-cadherin	1:200	3158029D
159Tb	CD68	1:400	3159035D
162Dy	CD8a	1:50	3162035D
165Ho	PD-1	1:50	3165039D
167Er	Granzyme B	1:100	3167021D
169Tm	Collagen 1	1:400	3169023D
170Er	CD3	1:50	3170019D
195/196/198Pt	ICSK1/2/3*	1:100	TIS-00001
191/193Ir	DNA 1/DNA 2	1:400	201192A

All stock antibodies are provided at 0.5 mg/mL.
Intercalator-Ir stock concentration is 125 µM.

Table 2. Custom Human Immuno-Oncology IMC Panel
(modified to exclude 3 markers and include 6 additional markers*)

Data acquisition and image rendering

For each tissue type, 2 serial sections mounted on the same slide were used to minimize the variability of staining from one slide to the next. Matching ROIs were ablated on the serial sections using the Hyperion and/or Hyperion+ Imaging Systems. ROI sizes were either 750 µm x 750 µm or 1,000 µm x 1,000 µm. Four replicates per tissue type were analyzed, where 1 replicate refers to a pair of matching ROIs.

Data were acquired using the Hyperion and/or Hyperion+ Imaging Systems, connected individually to the same Helios™, which houses the inductively coupled plasma time-of-flight (TOF) technology, the basis of CyTOF analysis. CyTOF Software v7.1 (compatible with both systems) was used for all data acquisitions. IMC data were visualized using MCD™ Viewer, and images of matching ROIs acquired on the Hyperion and/or Hyperion+ Imaging Systems were rendered using global thresholding (that is, the same threshold maximum value for a given channel).

Data analysis

S:N comparison of serial sections on the Hyperion or Hyperion+ Imaging System only.

As a control, to account for biological variability across serial sections, difference in signal between serial sections was evaluated by acquiring data on either the Hyperion or the Hyperion+ Imaging System only. MCD Viewer auto-threshold max (T-max) value, defined as the 98th percentile of all pixels in a single ROI, was designated as signal. Values obtained from MCD Viewer by manual selection of 3 regions, in which the antibody of interest was not expressed, were used for calculation of background noise. The overall change in S:N for a given channel was evaluated by calculating the ratio of S:N values for serial section 1 over S:N values for serial section 2. Two FFPE human tissues (Chronic Tonsillitis and Lymph Node Tumor) were studied, and 4 replicates per tissue type were analyzed.

S:N comparison of serial sections on the Hyperion Imaging System vs. the Hyperion+ Imaging System.

S:N ratios were calculated for data acquired using the Hyperion and Hyperion+ Imaging Systems. The S:N values for a given channel were calculated as described in the previous section. The overall change in S:N for a given channel was evaluated by calculating the ratios of S:N values for the Hyperion+ Imaging System over S:N values for the Hyperion Imaging System. Two FFPE human tissues (Chronic Tonsillitis and Lymph Node Tumor) were studied, and 4 replicates per tissue type were analyzed.

Cell segmentation

Cell segmentation was performed with the aid of the IMC Cell Segmentation Kit (ICSK) for improved nucleus and plasma membrane demarcation. Two conditions were evaluated: variability between serial sections only on the Hyperion Imaging System, and variability between serial sections on the Hyperion Imaging System vs. the Hyperion+ Imaging System. ilastik software was used for pixel classification using the 3 ICSK (195/196/198Pt) and 2 DNA (191/193Ir) channels, followed by employing the nuclear propagation strategy for cell segmentation using CellProfiler™ software. FFPE Human Prostate Cancer tissue was studied, and 4 replicates were analyzed.

Results

Image quality is maintained on the Hyperion+ Imaging System

There is no impact on the quality of images acquired on the Hyperion+ Imaging System as compared with those acquired on the Hyperion Imaging System. As visualized in Figures 1 and 2, matching ROIs acquired from serial sections had the same subcellular resolution and appeared equal by visual assessment.

Gain in S:N on the Hyperion+ Imaging System

Visual assessment: improved visualization of several markers.

Images of matching ROIs acquired on the Hyperion and Hyperion+ Imaging Systems were rendered using global thresholding. As observed in Figure 2, dim markers such as PD-1, PD-L1, FoxP3 and LAG-3 can be better visualized with the Hyperion+ Imaging System.

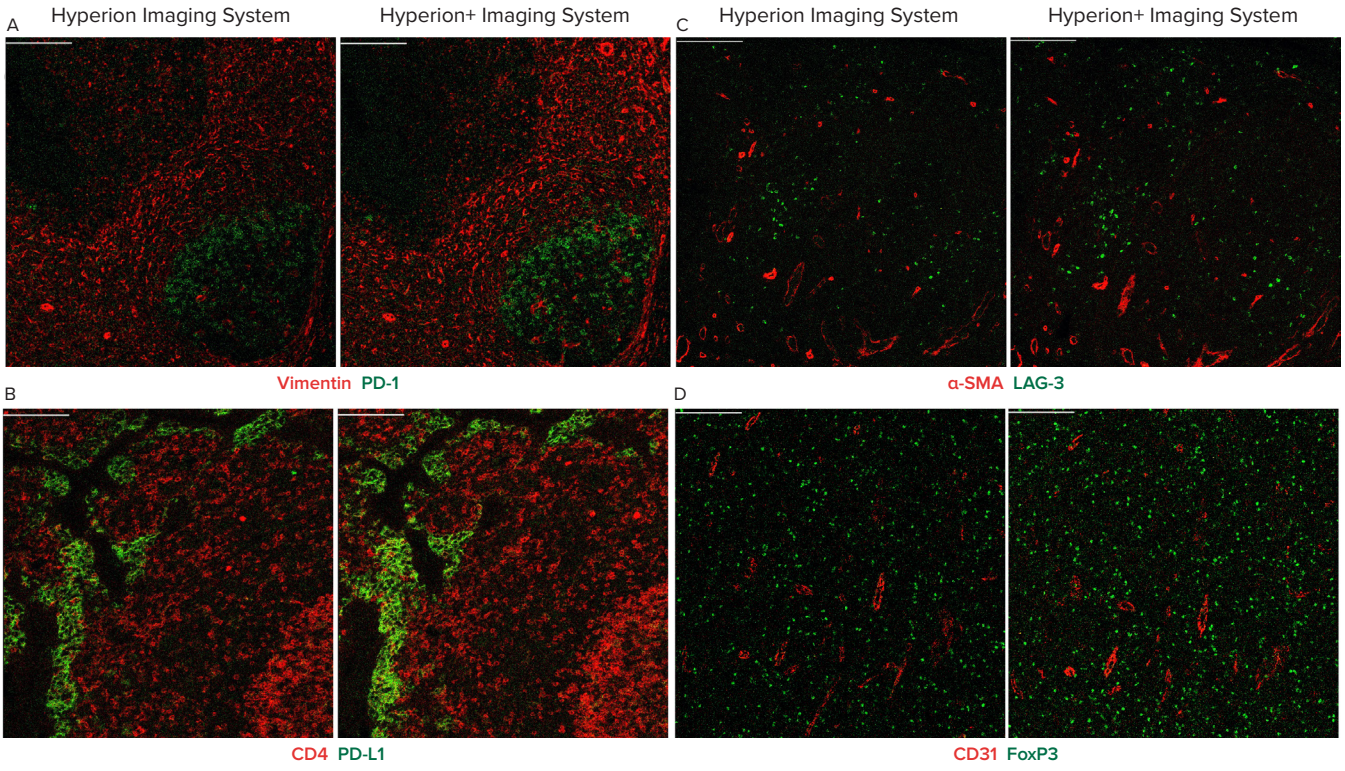

Figure 2. Dim markers can be better visualized on the Hyperion+ Imaging System. Comparison of FFPE human tissues examined by IMC using the Hyperion Imaging System vs. the Hyperion+ Imaging System. (A–B) FFPE Human Chronic Tonsillitis and (C–D) FFPE Human Lymph Node tumor tissues. Serial sections were stained with the antibody panel shown in Table 2, and matching ROIs were ablated using the Hyperion and Hyperion+ Imaging Systems. For comparison, a 2-channel image is shown, rendered using global thresholding. (A–B) ROI size = 750 µm x 750 µm, scale bar = 150 µm; (C–D) ROI size = 1,000 µm x 1,000 µm, scale bar = 200 µm.

Quantitative assessment: S:N ratio variability across serial sections is insignificant on the Hyperion or Hyperion+ Imaging System.

A control experiment to account for biological variability across serial sections was included. Matching ROIs on serial sections were ablated using either the Hyperion or Hyperion+ Imaging System only. A panel-wide (17 markers and 2 DNA channels) analysis of differences in S:N between serial sections was performed. As seen in Figures 3A and 3B, the variability of S:N across serial sections is negligible, whether using the Hyperion or the Hyperion+ Imaging System. Therefore, analysis of serial sections for S:N data comparison between the Hyperion and Hyperion+ Imaging Systems may be performed. Additionally, this experiment highlights the power of IMC in generating highly consistent data using serial sections, thus enabling users to easily scale up the number of unique markers they wish to identify simultaneously.

Quantitative assessment: increased S:N ratio on the Hyperion+ Imaging System.

The comparison of S:N ratio between the Hyperion and Hyperion+ Imaging Systems was performed by calculating the ratios of S:N values in the Hyperion+ Imaging System over S:N values in the Hyperion Imaging System for every channel. Depending on the expression level of a marker, a 5–55% gain in S:N was observed across all channels. Dim markers such as PD-1, PD-L1, FoxP3 and LAG-3 showed a 5–15% increase, while brighter markers including the DNA channels (191/193 Ir) showed a 20–55% improvement in S:N (Figure 3C). The gain in S:N observed using the Hyperion+ Imaging System, as compared with the Hyperion Imaging System (Figure 3C), reflects the improved limit of detection* of the Hyperion+ Imaging System.

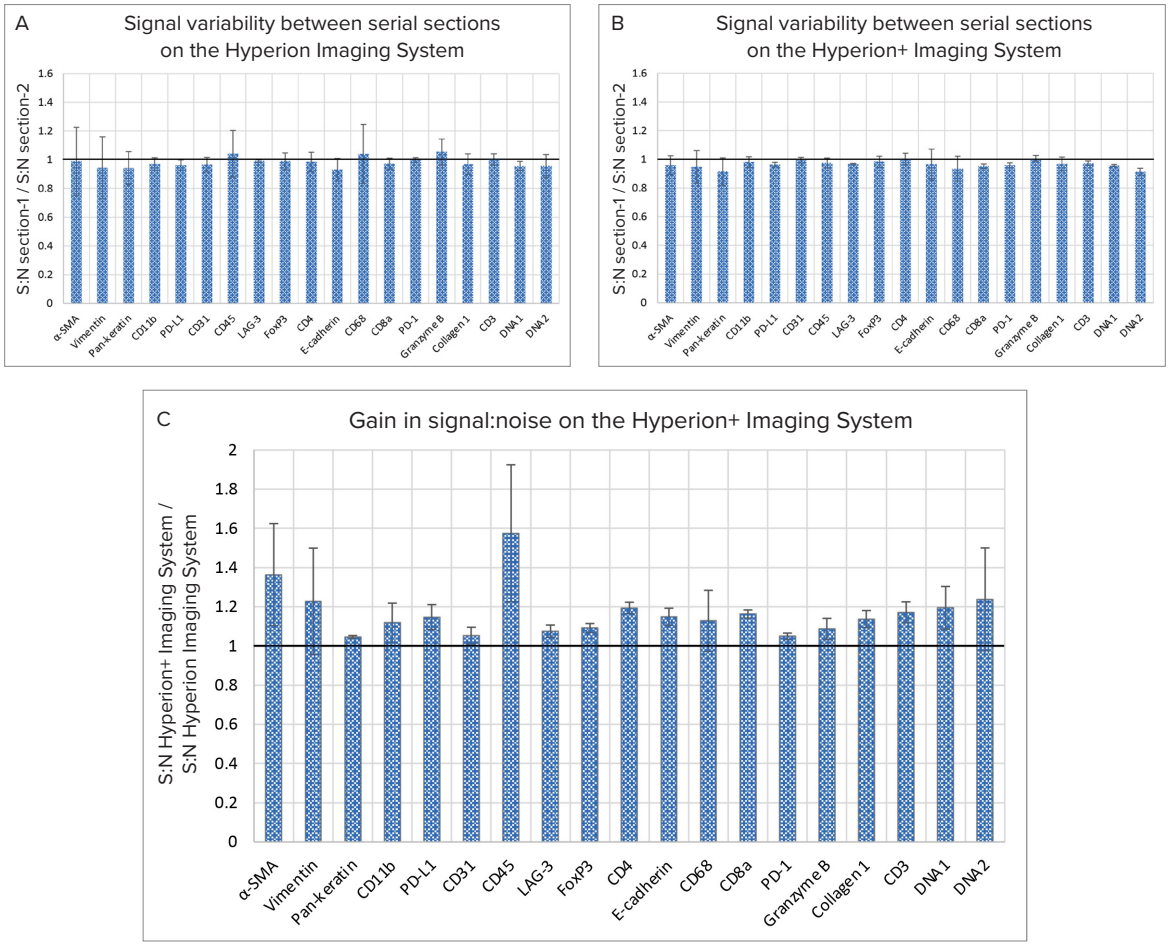

Figure 3. (A–B) S:N variability between serial sections is insignificant using either the Hyperion or the Hyperion+ Imaging System as quantitated by calculating the ratios of S:N values for serial section 1 over S:N values for serial section 2 for a given channel. **(C) Gain in S:N on the Hyperion+ Imaging System** was quantitated by calculating the ratios of S:N values for the Hyperion+ Imaging System over the S:N values for the Hyperion Imaging System for a given channel. FFPE Human Chronic Tonsillitis and Lymph Node tumor tissues were used for analysis.

* Limit of detection, described as the lowest analyte concentration required to produce a signal that is distinguishable from the noise level within a particular statistical confidence limit, can be estimated from the S:N ratio.

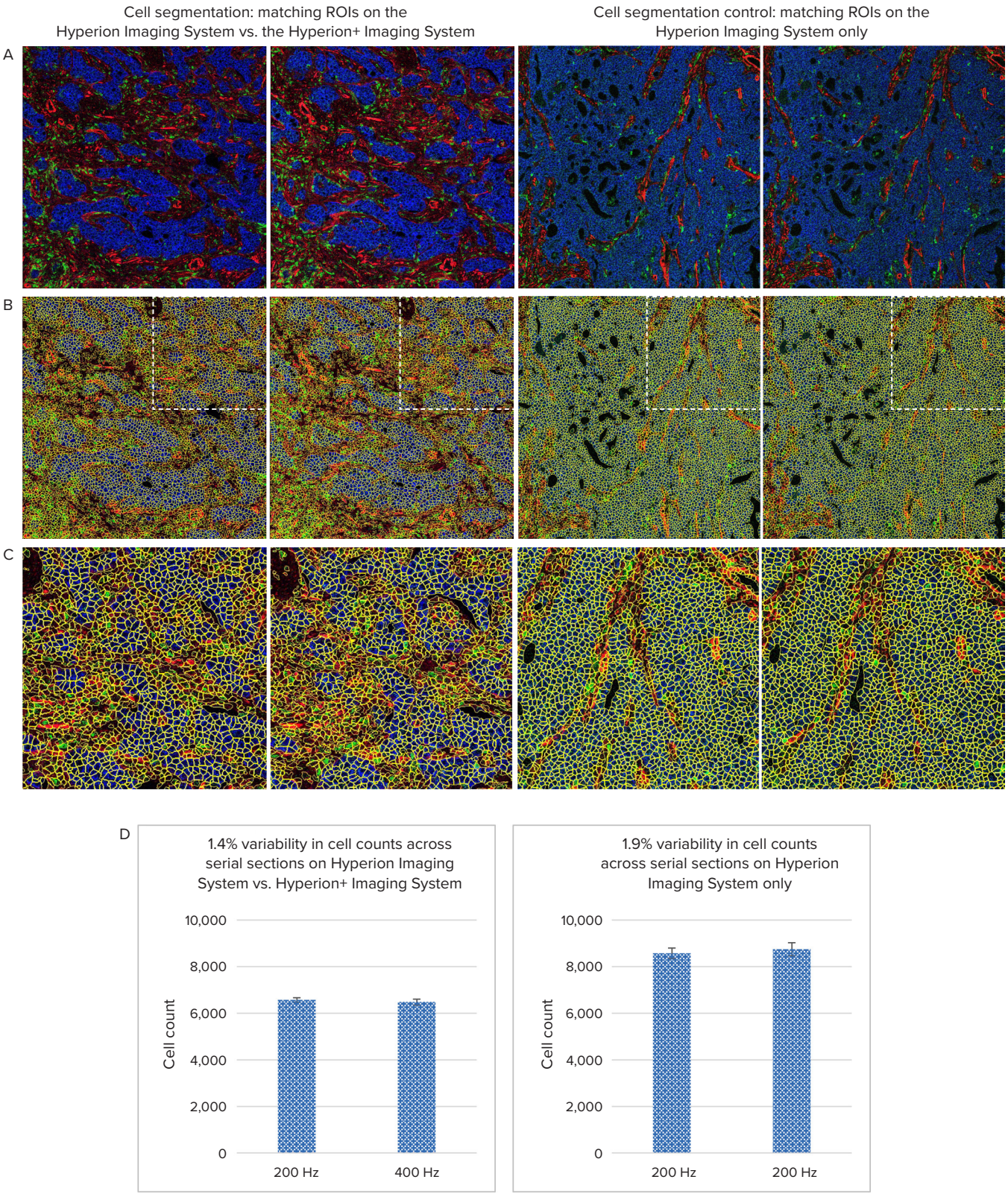

Figure 4. Comparison of cell segmentation between serial sections: Hyperion Imaging System vs. Hyperion+ Imaging System comparison (left), and the control experiment to account for biological variability among serial sections, using only the Hyperion Imaging System (right). (A) RGB images of FFPE Human Prostate Cancer tissue, with **aSMA**, **CD45** and **E-cadherin**. ROI size = 1,000 µm x 1,000 µm. (B) Cell segmentation overlaid on the RGB image. (C) Enlarged version of the selected area in panel B. (D) Variability in cell counts across serial sections on the Hyperion Imaging System vs. the Hyperion+ Imaging System (left) and on the Hyperion Imaging System only control (right).

Rigor of single-cell segmentation is maintained on the Hyperion+ Imaging System

There is no impact on the rigor of cell segmentation when images acquired on the Hyperion+ Imaging System are compared with those acquired on the Hyperion Imaging System. In Figure 4, the left panel compares matching ROIs acquired from serial sections using the Hyperion and Hyperion+ Imaging Systems. Cell segmentation showed equivalent number of cells, with only 1.4% variability. This variability is not greater than the 1.9% biological variability observed across serial sections when data are acquired only on the Hyperion Imaging System (control experiment, shown on right panel). The variability in cell counts between serial sections is minimal using both the Hyperion and the Hyperion+ Imaging Systems (Figure 4D). This result emphasizes the power of IMC in generating highly consistent segmentation data using serial sections and shows that the precision of single-cell segmentation is well preserved on the Hyperion+ Imaging System.

Conclusion

The second-generation Hyperion+ Imaging System has all the advantages of the Hyperion Imaging System with twice the speed. Even at the enhanced speed, image quality and accuracy of data analysis are well preserved. Additionally, several markers can be better visualized on the Hyperion+ Imaging System owing to the gain in S:N ratio as compared with the Hyperion Imaging System. These capabilities are key to rapidly uncovering important spatial interactions within the tissue microenvironment, thus accelerating the time to biomarker discovery and, therefore, the progress from bench to bedside.

Advantages of high-plex imaging using the Hyperion+ Imaging System

The Hyperion+ Imaging System helps you uncover important spatial relationships with high-plex imaging of 40-plus markers simultaneously at subcellular resolution. The key advantages:

- **Speed:** Acquire over 100 ROIs (1 mm^2) per week, getting to answers nearly twice as fast as with the Hyperion Imaging System.
- **Quality data:** Preservation of image quality and rigor of data analysis
- **Improved limit of detection:** Better visualization of several markers
- **Clean data:** Zero autofluorescence
- **Robustness:** Demonstrated data consistency using serial sections
- **Streamlined lab efficiency:** Straightforward stain-image-analyze workflow
- **Fewer complications:** No need for multiple staining and imaging cycles and elimination of tissue alterations due to chemical stripping or UV exposure
- **Easy panel design:** No need to optimize the order of labeling
- **Flexible panel expansion:** Ability to evolve from pre-designed panels
- **Expert support:** Field scientists and engineers deliver personalized assistance to ensure success.

Materials

Protocol

The Imaging Mass Cytometry Staining Protocol for FFPE Sections (400322) can be downloaded from standardbio.com. For a full list of antibodies available for IMC, visit **store.fluidigm.com**.

Required Materials from Standard BioTools™

Product Name	Catalog Number
Maxpar® Human Immuno-Oncology IMC Panel Kit	201505
IMC™ Cell Segmentation Kit	TIS-00001
Cell-ID™ Intercalator-Ir	201192A
Anti-CD11b- 149Sm	3149028D
Anti-CD31- 151Eu	3151025D
Anti-CD223 (LAG-3)- 153Eu	3153028D

Materials Used from Other Suppliers

Product Name	Source
FFPE Human Chronic Tonsillitis slide	US Biomax (Cat. No. HuDAT188)
FFPE Human Lymph Node Tumor slide	US Biomax (Cat. No. HuCAT436)
FFPE Human Prostate Cancer slide	US Biomax (Cat. No. HuCAT367)
ilastik software v1.3.3	ilastik.org
CellProfiler software v4.2.1	cellprofiler.org

Learn more at **fluidigm.com/hyperion-plus**

Or contact: **fluidigm.com/tech-support**

CORPORATE HEADQUARTERS
2 Tower Place, Suite 2000
South San Francisco, CA 94080 USA
Toll-free: 866 359 4354 in the US and Canada
Fax: 650 871 7152
standardbio.com

SALES
North America | +1 650 266 6170 | info-us@fluidigm.com
Europe/EMEA | +33 1 60 92 42 40 | info-europe@fluidigm.com
Latin America | +1 650 266 6170 | info-latinamerica@fluidigm.com
Japan | +81 3 3662 2150 | info-japan@fluidigm.com
China (excluding Hong Kong/Macau) | +86 21 3255 8368 | info-china@fluidigm.com
All other Asia-Pacific countries | +1 650 266 6170 | info-asia@fluidigm.com

For Research Use Only. Not for use in diagnostic procedures.

FLDM-00968 Rev 01